Research Article

For reprint orders, please contact: reprints@future-science.com

Therapeutic Delivery

# Development of a dry powder for inhalation of nanoparticles codelivering Active Ingredient and *ABCC3* siRNA in lung cancer

Vivek Patel*[,1], Denish Bardoliwala[1], Rohan Lalani[1], Sushilkumar Patil[1], Saikat Ghosh[1], Ankit Javia[1] & Ambikanandan Misra[1,2]

[1]Department of Pharmaceutics, Faculty of Pharmacy, Kalabhavan Campus, The Maharaja Sayajirao University of Baroda, Vadodara, Gujarat, 390001, India

[2]Shobhaben Pratapbhai Patel School of Pharmacy & Technology Management, SVKM's NMIMS University, Mumbai, Maharashtra, 400056, India

*Author for correspondence: vnpatel.2902@gmail.com

**Background:** The current study sought to formulate a dry powder inhalant (DPI) for pulmonary delivery of lipopolymeric nanoparticles (LPNs) consisting of Active Ingredient and siRNA for multidrug-resistant lung cancer. siRNA against ABCC3 gene was used to silence drug efflux promoter. **Results & discussion:** The formulation was optimized through the quality by design system by nanoparticle size and Active Ingredient entrapment. The lipid concentration, polymer concentration and lipid molar ratio were selected as variables. The DPI was characterized by *in vitro* deposition study using the Anderson cascade impactor. DPI formulation showed improved pulmonary pharmacokinetic parameters of Active Ingredient with higher residence time in lungs. **Conclusion:** Local delivery of siRNA and Active Ingredient to the lung tissue resulted into an enhanced therapeutic effectiveness in combating drug resistance.

**Graphical abstract:**

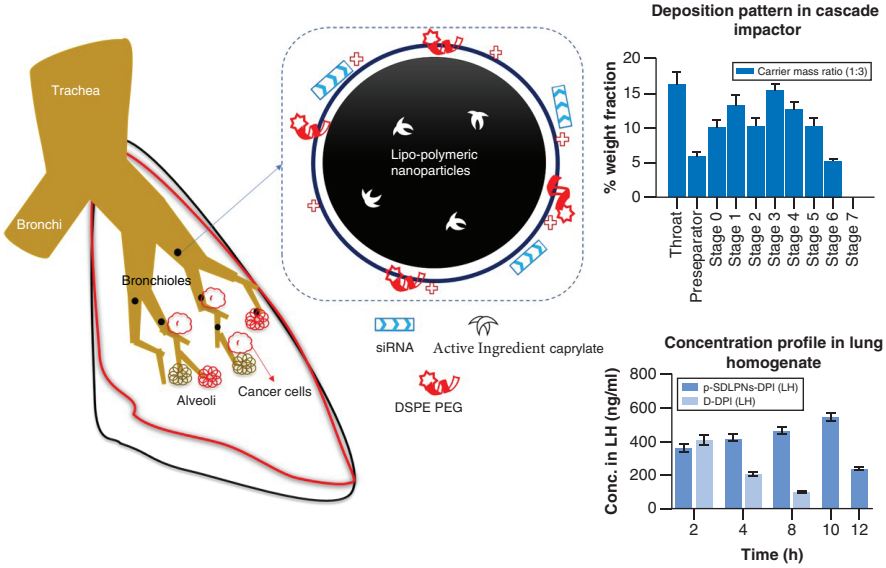


First draft submitted: 22 September 2020; Accepted for publication: 13 July 2021; Published online: 10 August 2021

**Keywords:** chemosensitization • Active Ingredient • Cryo-TEM • DPI • gene knockdown • lung cancer • MTT assay • PERT-PCR • siRNA

newlands press

Lung cancer is one of the principal causes of mortality, comprising a quarter of all cancer-related deaths [1]. The primary treatment and supportive care is done by administering chemotherapeutic agents via oral as well as parenteral routes. The treatment alternatives include either oral or intravenous delivery of chemotherapeutics in combination with radiation therapy and surgery [2]. Orally delivered chemotherapeutic agents exhibit poor bioavailability owing to significant first pass metabolism, and further the bioavailable dose may lead to non-tumor-cell toxicity as well. The optimal therapy for lung cancer would be to locally deliver high-dose therapeutics to lung tumor tissues through an inhalation route to maximize treatment efficacy and minimize adverse effects due to systemic absorption. The lung's vast surface area for deposition of aerosolized therapeutics, avoidance of first-pass hepatic metabolism and limited permeation of inhaled therapeutics into systemic circulation are the primary advantages associated with pulmonary administration of therapeutics thereby increasing therapeutic index of drug.

Development of drug resistance is a key reason for failure of chemotherapy. The activation of protein efflux pump among membrane transporters pumps out the drugs from cells leading to decline in treatment efficacy [3]. It is well established that RNA interference (RNAi) technology can be successfully utilized for inhibition of proteins accountable for resistance [3–5]. Several genes such as *p-gp*/*MDR1*, *ABCB2*, *ABCC1*, *ABCC2* and *ABCC3* have been recognized enhancing resistance among different antineoplastic agents. Silencing the specific gene responsible for drug resistance is now a widely explored concept among researchers to develop efficacious treatment [6]. Expressions of ABCC3 efflux proteins are observed to be higher in lung cancer cells.

Use of cotreatment approach by using therapeutics agents having different mechanism of action in cancer cells would be more effective than monotherapy or chemotherapy in decreasing the occurrences of resistance and improve therapeutic outcome [2]. A combination treatment approach involving chemotherapy and gene/siRNA therapy may prove effective compared with the individual components in cancer treatment [7–9]. This strategy is referred to as chemosensitization, wherein the efficiency of therapeutic agent is improved by knockdown of multidrug-resistant (MDR) genes by use of RNAi technology [10–12]. Therefore, development of a nanomedicine formulation capable of delivering an anticancer drug and siRNA via the pulmonary route for treatment of lung cancer is highly beneficial [12–18].

A variety of nanocarriers have been formulated for pulmonary delivery of therapeutics [19–21]. Liposomes and polymeric nanoparticles, for example, are delivery systems with several successful products (Active Ingredient, Active Ingredient, Active Ingredient, Marqibo, Active Ingredient and Active Ingredient) on the market. They have the ability to carry drug and gene therapeu-tics as well. Liposomes exhibit biocompatibility, biofunctionality and a superior pharmacokinetic profile, whereas nanoparticles possess properties such as mechanical stability, chemical tunability, higher drug loading and a sus-tained release drug profile [22]. Therefore, there is ample motivation to develop a formulation approach that brings together these properties, thereby diminishing disadvantages such as incomplete drug loading and storage stability issues [3,23,24]. Lipopolymeric hybrid nanoparticulate carrier systems possess properties such as low toxicity, bio-compatibility, loading of diverse ranges of therapeutics, increasing selectivity of cancerous cells by conjugation with targeting ligand and selective extravasations in tumor cells due to size characteristics and enhanced permeability and retention effects [25].

In the current work, we hypothesized that silencing the MDR gene *ABCC3* (MRP3) through siRNA (RNA interference technology) would improve the effectiveness of chemotherapy by diminishing cancer cell resistance [26,27]. A simple thin film hydration method was employed to formulate lipopolymeric nanoparticles (LPNs) by using PEG-PLA as a block copolymer for drug entrapment and as a matrix to provide structural rigidity to the carrier, DOTAP as cationic lipid for siRNA complexation and DSPE-PEG 2000 for PEGylation of LPNs to provide stealth nature and also minimizing the hypersensitivity reactions. Dry powder for inhalation (DPI) of ABCC3 siRNA complexed Active Ingredient-loaded LPNs were formulated using lyophilization with an inhalable carrier. The aerodynamic properties of the processed lyophilized bulk were assessed through the Anderson cascade impactor [24,28,29]. A particle aerody-namic diameter between 1 and 5 μm has been reported for successful inhalational delivery of a nano-formulation. Particles <1 μm are exhaled, whereas those >5 μm are deposited in the upper part of trachea instead of the bronchi/bronchioles or alveolar part of lung [17]. Because of the higher stability of the lipids in dry powder form, the DPI mode of delivery was preferred over nebulization and metered dose inhalation (MDI). The targets for the finished DPI product were to obtain a dry powder with optimized features for deposition into the lower airways with minimal changes to the size and efficacy of LPNs during the lyophilization process and to assess the performance of the designed formulation in cancer cell lines. A thin film hydration manufacturing method to formulate LPNs had

already been developed and optimized in our previous work [30], and the same method was adapted for the current work with additional manufacturing steps for DPI preparation. The lyophilization and subsequent mixing with inhalation carrier were performed on LPN preparation to produce the DPI. Further *in vitro* pulmonary deposition and pulmonary pharmacokinetic studies were conducted to evaluate DPI performance.

## Materials & methods

### Materials

PEG-PLA Mn 2000 was procured from Sigma-Aldrich (Bengaluru, India). DPPC, DOPE, DOTAP and cholesterol were from Lipoid GmbH (Ludwigshafen, Germany). DSPE-PEG (2000) was procured from Avanti Polar Lipids (AL, USA). ABCC3 (MRP3) siRNA (20–25 nucleotide) was purchased from Santacruz Biotechnology Inc. (CA, USA). The nucleotide sequence for ABCC3 siRNA forward primer was ATGAAGTCTGCCATGAGGGG (5′→3′) and reverse primer was CCCTGGACCCTGTAACACTC (5′→3′). siRNA solution was obtained as per manufacturer protocol to get 10 µM solution upon reconstitution from vial of 3 nmol lyophilized siRNA. Supporting reagents for transfection studies: Unconjugated control (scrambled) siRNA, FITC-conjugated control, siRNA transfection medium, siRNA dilution buffer and siRNA transfection reagent were obtained from Santacruz Biotechnology Inc. USA. Eurofins Scientific (Bengaluru, India) provided forward and reverse primers for cDNA amplification of ABCC3 gene of high purity (salt free) grade through custom synthesis. The forward primer sequence was AGGGAGTGTTACAGGGTCCA (5′→3′), and GGTACCAAGGCCACAGTTCT (5′→3′) was reverse primer. The base-pair sequences were determined by with the NCBI-BLAST method. Trypsin EDTA, DAPI, fetal bovine serum (FBS), EtBr, Dulbecco's minimum Eagle medium (DMEM), MTT, propidium iodide (PI) and antibiotic solution 100× liquid (Active Ingredient and Active Ingredient) were purchased from Himedia (Mumbai, In-dia). DEPC-treated (nuclease free) apparatus, tips and tubes were used, and molecular-biology grade solvents such as chloroform and methanol were used for experiments.

#### *Cell culture*

The lung adenocarcinoma A549 cells were cultivated and maintained in DMEM supplemented with 10% FBS and 1% solution Active Ingredient and Active Ingredient solution. The cell line was purchased from National Center for Cell Science, Department of Biotechnology, government of India. The cell cultures were incubated in 5% $CO_2$ in a humidified atmosphere (Jouan IGO150 CELL life $CO_2$ Incubator, Thermo Fisher Scientific, Mumbai, India) at 37°C temperature. T-25 cell culture flasks were used to cultivate and preserve cells as monolayer culture twice every week.

### Formulation & physical-chemical characterization of drug-loaded lipopolymeric nanoparticles

#### *Formulation & optimization of drug-loaded lipopolymeric nanoparticles*

LPNs were manufactured using thin lipo-polymeric film formation through hydration and extrusion. Primary lipid (DPPC), secondary lipids (DOTAP, DOPE and polymer (PEG-PLA; 5 mg/ml) were dissolved in chloroform in required ratio in a flask. Box-Behnken design (BBD) matrix was generated by means of Design Expert 7.0 software (State Ease, MN, USA). The design had 15 experimental runs. BBD was selected over other DoE designs because it requires fewer runs and has good predictability within the spherical design space, suitable for evaluating quadratic response surfaces. Lipid concentration, polymer concentration and lipid molar ratio were considered independent variables. Nanoparticles size and Active Ingredient caprylate entrapment efficiency amount in LNPs were taken as dependent (response) variables [31]. The lipopolymeric film was produced by organic solvent evaporation by nitrogen gas flushing until a thin film was observed. The film was dried in a vacuum desiccator overnight to eliminate residual solvent at 100 mm Hg and 25°C. The phosphate-buffered saline (PBS) pH 7.4 was used for film hydration on water bath at 45°C for 15 min. Then complete hydration was achieved through bath sonication for 15 min at 45°C. In the hydration step, Active Ingredient caprylate (1 mg/ml) was dissolved in PBS pH 7.4. A Genizer high-pressure liposome extruder was used to extrude the hydrated vesicles five times at 250 psi through 200-nm polycarbonate membranes (the extrusion process was accelerated by a polyethylene drain disk, which supported the polycarbonate membrane) to form monodisperse and unilamellar LPNs. The postinsertion method was used to integrate DSPE-PEG 2000 (3 mol % of total lipid contents) into preformulated LPN aqueous dispersion. This was mixed lower than the critical micellar concentration (CMC) level to LPN aqueous dispersion in a water bath at glass transition temperature (42°C) under gentle agitation to obtain PEGylated drug-loaded lipopolymeric nanoparticles (p-DLPNs) [28,32].

Quasi-elastic laser light scattering was used to determine polydispersity index, LPN size (diameter, nm) and surface charge (zeta potential, mV) using a Zeta PALS dynamic light scattering detector (15-mW laser, incident beam $\frac{1}{4}$ 676 nm) (Malvern zetasizer Nano ZS, Malvern Instruments, Malvern, UK) at room temperature. Viscosity and refraction indices values were put identical to values of water. The ultracentrifugation method was used to assess drug entrapment efficiency and drug loading for separation of free drug from LPNs. For this, 1 ml of p-DLPNs were taken in a 2-ml micro-centrifuge tube. The tubes were centrifuged at 15,000 rpm (*g* value: 25,200) at 10°C for 30 min to settle the free Active Ingredient caprylate and unutilized polymer and lipid at the bottom of the centrifuge tube. The supernatant containing LNPs were collected in a separate vial. The entrapped drug was determined by analyzing supernatant after centrifugation as per Equation 1. The amount of entrapped drug and in 1 ml formulation was determined by O-phenylenediamine (OPDA) derivatization wherein dilutions were made using methanol:acetonitrile (1:2) and estimated at 705 nm with UV-visible spectrophotometer as formerly reported [33]. The drug loading calculation was carried out as per Equation 2.

$$\%\ \textit{Entrapment efficiency} = \left[\frac{\text{Entrapped Active Ingredient}}{\text{Total Active Ingredient}}\right] \times 100 \qquad \text{(Eq. 1)}$$

$$\%\ \textit{Drug loading} = \frac{\text{Entrapped Active Ingredient}}{\text{Total lipid and polymer} + \text{total Active Ingredeint}} \times 100 \qquad \text{(Eq. 2)}$$

### *In vitro dissolution & drug release kinetics*

The drug release for optimized p-DLPNs were assessed in three media with pH values of 5.5 (acetate buffer saline), 6.6 (PBS) and 7.4 (PBS) to mimic the physiological conditions in cancer cells, tumor interstitium and blood/normal tissues, respectively. Dialysis bag (Dialysis Membrane-70, molecular weight cutoff 7000 Da, Himedia) was activated and used for a drug release study in 100-ml dialysis media. 1-ml aliquots from the receptor compartment were sampled from the beaker into 1.5-ml Eppendorf tubes at regular time intervals up to 96 h and replaced with an equal quantity of fresh media each time. The Active Ingredient caprylate amount in the aliquots was estimated using OPDA derivatization by UV-visible spectroscopy at 705 nm, and cumulative release was calculated. Drug release data were integrated in different kinetic models (zero order, first order, Hixon–Crowell model, Korsmeyer–Peppas and Higuchi) to determine the release kinetic pattern from the p-DLPNs [28].

## Formulation & development of siRNA complexed p-DLPNs

### *Formulation of p-SDLPNs & siRNA complexation efficiency*

DLPNs were formulated as per procedure described in section 'Formulation and optimization of DLPNs'. However, PBS pH 7.4 prepared using nuclease-free water (NFW; DEPC treated) was used for hydration of lipopolymeric film. siRNA complexation with cationic LPNs was defined by the nitrogen:phosphate (N/P) ratio wherein N indicates the number of quaternary nitrogen of the cationic lipid (DOTAP) and P indicates the number of phosphate group of siRNA nucleic acid base. Preparation of p-DLPNs and siRNA (p-SDLPNs) was done in two steps. The first step involved incubation of naked siRNA (100 nM) with preformed DLPNs at various N:P charge ratio, ranging from 0 to 4 (increments of 1) to obtain SDLPNs. The mixture vortexing was done for 2 min and incubated for different periods of time (10, 20, 30, 60 and 120 min) and at different temperatures (5–35°C, increments of 10°C) to select the optimal processing condition. The second step employed the postinsertion method for DSPE-PEG 2000 (3 mol % of total lipid contents) incorporation into preformulated SDLPN aqueous dispersion as per the procedure described in section 'Formulation and optimization of DLPNs' to obtain p-SDLPNs [2].

The siRNA complexation with DLPNs at different N/P ratio was assessed by agarose gel electrophoresis. Briefly, p-SDLPN samples were mixed with 2 µl of 6× DNA gel loading buffer (Thermo Fisher Scientific, USA) and loaded onto a 2% agarose gel having 0.5 µg/ml ethidium bromide. The Electrophoresis was carried out at 100 V for 20 min in TBE (10.8 g/l TRIS base, 5.5 g/l boric acid, 0.58 g/l EDTA) buffer. The UV trans-illumination & Gel Doc System (Bio-Rad, CA, USA) was used to capture siRNA band images. The complexation efficiency of siRNA with DLPNs was measured by centrifugal assay. P-SDLPNs samples at different N/P ratio were centrifuged at for 30 min at 25000 rpm and 4°C. NanoDrop UV Spectrophotometer (Thermo Fisher Scientific) was used to analyze siRNA content after separation of the aqueous supernatant layer.

### *Measurements of size & zeta potential*

Average particle size and zeta potential tests were carried out using p-SDLNPs as per procedure described in section 'Formulation and optimization of DLPNs'. The particle size was checked with respect to the postinsertion PEGylation step effect. Formulation dilutions were done with 10 mM of phosphate buffer prepared using NFW before measurement.

### *Cryo & freeze fracture transmission electron microscopy*

Size and morphological evaluations of LPNs were done using cryo-TEM (TECNAI G2 Spirit BioT WIN, FEI, Eindhoven, The Netherlands) functioning at 200 kV with a resolution of 0.27 nm. The glow discharge method was used to change the hydrophobic grid to hydrophilic, then p-SDLPNs were placed on the grid and cryofrozen in liquid ethane at -180°C. A cryo holder was used to hold the grid and inserted into a microscope. Images were captured at 70,000× magnification.

In freeze fracture transmission electron microscopy (TEM) study, a gold grid spacer was used to sandwich a 2-µl sample between copper plates. Samples were quickly frozen in liquid ethane at -180°C, and a freeze fracturing apparatus (BAL-TEC Inc., Balzers, Liechtenstein) was used to fracture the samples at -150°C with $2 \times 10^{-7}$ mbar pressure. Samples were enclosed at different angles with Pt/C grid and observed by a Philips EM 301 microscope [34].

## Development of DPI for p-SDLPNs

### *Preparation of p-SDLPNs-DPI*

p-SDLPNs were prepared in NFW to which different cryoprotectants (e.g., Active Ingredient, lactose and trehalose) were added separately for evaluation and filled in type 1 borosilicate glass. Formulations were subjected to lyophilization (Virtis Advantage Plus Lyophilizer, CA, USA), and the cycle was set to freeze at -40°C for 6 h, with primary drying at -20°C for 12 h and secondary drying at 25°C for 24 h under the vacuum with required ramping and holding. The cake was evaluated organoleptically, and the lyophilized vials were stored at 2–8°C until further use. The lyophilized cake was passed through a sieve (120# and 230#) sequentially to convert the cake into a fine powder. Fine-powder particle size was evaluated by the Malvern Mastersizer 2000. The obtained lyophilized powder formulation was mixed manually using the geometric dilution method with the inhalational carriers (Inhalac-230 and Respitose-SV003) having characteristic flow properties to obtain p-SDLPNs-DPI. Lyophilized powder formulation to carrier mass ratio ranging from 1:1 to 1:5 were tested, and the optimal batch was selected based on improved dispersibility of the DPI during inhalation and solid-state characteristics. Powder processing was carried out in a room with a relative humidity ≤30%. The p-SDLPNs-DPI were filled in a size 3 capsule to study aerodynamic behavior. Moisture content analysis was done by the Karl–Fischer titration method [16].

### *In vitro deposition tests by the Anderson cascade impactor*

The Anderson cascade impactor (Copley Scientific, Nottingham, UK) was used to measure the aerodynamic properties of p-SDLPNs-DPI. Powders for inhalation were filled in size 3 capsules. The capsules were fitted into actuators (Ciplahaler, Mumbai, India) for the dispersion of the powder into cascade impactor. Ciplahaler is MDI made of a canister of pressurized medication that fits into a plastic actuator sleeve and connects to the mouthpiece. To mimic human respiration behavior, flow rate was set to the 60 l/min for 4 s so that a volume of 4 l is drawn though the inhaler, creating a 4-kPa pressure drop. The amount of drug deposited on the induction port, preseparator, plates, sieves and powder left behind in the capsule and inhaler device were collected with a minimal amount of methanol to prevent excessive dilution. The collected fractions of all the sieves and plates were analyzed for active ingredient content. Mass median aerodynamic diameter (MMAD), emitted dose (ED), recovered dose (RD), fine powder fraction (FPF) [35] and geometric standard deviation parameters were calculated according to USP 41 NF 36 [36].

### *Powder x-ray diffraction*

The x-ray diffraction styles of the active ingredient powder and p-SDLPNs-DPI were obtained using an x-ray diffractometer (Rigaku-Micro007, Tokyo, Japan) with a 1.2-kW generator, image plate detector of 345 mm plate diameter and a usable detector area of 93.480 $mm^2$. The x-ray diffractometer was run with a 30-mA anode current having 40-kV accelerating voltage. The samples were smoothly put on an aluminium tray using a glass slide and exposed to target of CuKα-15,418-Å radiation source. The powder x-ray diffraction pattern was collected from diffraction angles 2 theta values between 4 to 40°.

### *Integrity of siRNA*

Evaluation of siRNA integrity in formulated p-SDLPNs-DPI was done to verify the amount of complexed siRNA compared with siRNA added after its conversion to powder form for inhalation. The estimation was performed using the gel electrophoresis densitometry method. DEPC-treated water was used to dilute p-SDLPNs-DPI to prepare 100 µl final volume. Two hundred microliters of phenol/chloroform (1:1 v/v) was used for vortexing and spun with 14,000 rpm speed for 30 min at 4°C. The aqueous layer was separated to analyze complexation efficiency from centrifuged samples using NanoDrop UV Spectrophotometer (Thermo Fisher Scientific). Furthermore, 5 µl of loading buffer was mixed with the aqueous layer, and the mixture was loaded onto 2% agarose gel. Gel photopgraphy and UV trans-illumination using a Gel Doc System (Bio-Rad) were used to capture siRNA bands images [37].

## *In vitro* cell line studies

### *Cytotoxicity study by MTT assay*

Cytotoxicity assessment for the LPNs was carried out using MTT assay. A lung adenocarcinoma cell line (A549) was selected and seeded at a density of $5 \times 10^3$ cells per well in 96-well plate. After 24 h, the cells were treated with p-DLPNs, p-SDLPNs, redispersed p-SDLPNs-DPI (redispersed LPNs) at various concentrations (0.1–500 µM) of drug solution (Dsol) (1 mg/ml in 0.9% Nacl) in DMEM containing FBS (10%) with antibiotic (Active Ingredient/Active Ingredient 0.1%) solution. The plates were then incubated at 37°C. After a period of 6 h, the transfection medium was removed from the plates, and fresh complete medium was added. Further incubation for a period of up to 3 days was carried out with replacement of spent medium every 24 h. At the end of the specific incubation period, each well was washed with PBS, and MTT (50 µl of 1 mg/ml) solution was added to them, followed by 4-h incubation in the dark. The medium was then removed, and DMSO (200 µl) was added to each well and evaluated using an ELISA microplate reader (Bio-Rad; absorbance: 570 nm, reference filter: 655 nm) taking untreated cells as negative control and Triton ×100 (0.5%) as a positive control. To evaluate nanocarrier toxicity, blank LPNs (with concentration equivalent to $10^3$ µM drug load – twice the highest concentration tested in the study) were also included. Cell viability data were then plotted and inhibitory concentration ($IC_{50}$) calculated using GraphPad prism 7.0 software (using the dose–response inhibition normalized nonlinear regression model), and fold change in $IC_{50}$ values was determined [38].

### *Gene knockdown by real-time PCR*

To quantitatively estimate the knockdown of mRNA by siRNA, real-time (RT)-PCR was used. Cells (A-549) were seeded onto 24-well plates at a density of $5 \times 10^4$ cells/well. Optimized formulation of p-SDLPNs was added to each well after 80% confluency. siRNA at concentrations of 50, 100 and 200 nM were used. Transfection of cells with lipofectamine 2000 (L2K) according to the manufacturer's instruction as a positive control and scrambled sequence (NC-siRNA) of siRNA were carried out to check sequence specificity, along with an untreated control to assess gene expression. After 48 h, TRIzol reagent (Invitrogen, MA, USA) was used to isolate RNA from cells and reverse transcribed into cDNA using cDNA conversion kit (Invitrogen). The mRNA level was quantified using Step One RT-PCR (Applied Biosciences, UT, USA). Each reaction contained primers (forward and reverse), and cDNA (2 ng) and SYBR Green Master mix (Applied Biosciences), in a volume of 20 µl. The GAPDH was used to normalize mRNA expression level [39].

## *In vivo* studies

Laboratory animals were handled with care by following institutional and national guidelines. The experiments and protocols were approved by the Institutional Animal Ethical Committee of Maliba Pharmacy College, Uka Tarsadia University, Bardoli. The protocol number was MPC/IAEC/02/2019. The studies were also approved by the committee tasked with control and supervision of experiments on animals, Ministry of Social Justice and Empowerment, Government of India.

### *Pulmonary pharmacokinetics*

Albino rats were acclimatized to 12 h day/light pattern with supply of water and commercial rodent diet. Intraperitoneal injection of 5 mg/kg xylazine and 50 mg/kg ketamine were given to anesthetize animals. Surgery was done to expose the trachea on the ventral side of the rat neck, and a 20# needle was used for tracheal puncturing just beneath larynx. Animals were separated into two experimental groups (six rats each group), and intratracheal

doses were given: DPI-D for group 1 and p-SDLPNs-DPI for group 2 (dose of 200 μg Active Ingredient and 50 μg siRNA equivalent DPI formulation). Bronchoalveolar lavage (BAL) [32] was carried out on anesthetized and cannulated animals (Sprague-Dawley rats) with 12 ml ice-cold PBS. Cannulated PE200 tubing was used to inject 12 ml of PBS into the lung via one syringe, and the other syringe was used to withdraw BAL by gentle aspiration. Centrifugation was done for 10 min at 1500 rpm using 8–9 ml BAL liquid. 4 ml of supernatant was separated and stored at
-20°C. The remaining supernatant was mixed with 10% Triton ×100 at a ratio of 9:1 to dissolve the LPNs and assayed by inductively coupled plasma atomic emission spectroscopy (Labtam, Victoria, Australia; model 8440) to analyze platinum content (molecular weight of Active ingredient is 300.1 g/mol and platinum 195.1 g/mol, hence 1.5381 μg of Active Ingredient = 1 μg platinum). The part of trachea underneath the site of instillation and the lungs were excised and homogenized in 10 ml PBS containing 1% Triton x100, and the diffused drug was analyzed. The drug concentration in the lung was the drug estimated in lung homogenate [19] as well as BAL fluid and pulmonary pharmacokinetic parameters ($C_{max}$, $T_{max}$, area under the curve, $t_{1/2}$ and mean residence time [MRT]) were calculated [36].

### *Enzymatic activity estimation*

Albino rats were separated into four experimental groups (six rats each group) and doses (dose of 200 μg Active Ingredient and 50 μg siRNA equivalent DPI formulation) were given as: (1) saline, (2) DPI-D (3) p-SDLPNs-DPI (4) 0.1 μg/ml lipopolysaccharides (positive control) with similar procedure described in section 'Pulmonary pharmacokinetics'. Animals were euthanized by overdose of phenobarbital (75 mg/ml) i.p. injection after 24 h of administration. BAL was performed according to procedure described earlier, and the supernatant was separated from the BAL fluid. From this supernatant, the enzymatic activity of alkaline phosphatase (ALP) and lactate dehydrogenase (LDH) were estimated using commercially available kits (Abcam, Mumbai, India). Enzyme level in the BAL fluid was recorded as fold increments compared with saline-treated groups. Lungs were then surgically removed, and the right lung was gently detached from the trachea, heart, bronchus, thymic tissue and any former adherent clot or fibrinous exudates. The calibrated scale was used to weigh isolated right lung tissue and lung weight to body weight (lung weight:body weight) ratio was estimated. Weight of lungs were reported as g/100 g body weight [40].

### Statistics analysis

Experiments were designed in triplicate. Data are articulated as the mean ± standard deviation (SD) unless otherwise specified. The statistical significance of the results was determined using Student's t-test ($p < 0.05$), and one-way analyses of variance [41] were run to check statistical significance.

## Results & discussions

### Formulation & evaluation of DLPNs

#### *Formulation & optimization of DLPNs*

LPNs were formulated by the film hydration method followed by extrusion [29]. After thin lipopolymeric film formation and hydration, these sheet fold upon to form vesicles. Lipids and the diblock copolymer self-assemble according to the hydrophobic interaction to decrease surface free energy of hybrid system. DSPE-PEG molecules are suggested to participate in this self-assembly process, providing an outer layer to LPNs and protecting them from pulmonary immune attack, thus conferring stability to this hybrid system [42,43]. Various drugs can be encapsulated by PEG-PLA polymer due to its amphiphilic nature, which forms a solid matrix core inside LPNs [44]. Hydrating the lipopolymeric film beyond the lipid mixture's phase transition temperature and sonication aid in the self-assembly process of LPN formation. DPPC (glass transition temperature 41°C) was used as a primary lipid to form a hybrid nanoconstruct [45]. The neutral lipid DOPE assists endosomal escape of nanocarrier. DOPE's fatty acid carboxyl ions impart stability to the nanocarrier in the lamellar phase in neutral pH due to electrostatic repulsion, but they are converted into unstable the hexagonal phase in the endosome's acidic pH due to protonation of these groups. The cargo is released into the cytosol after fusion and aggregation [46]. Moreover, the cationic charges to LPNs were generated by addition of DOTAP to ensure effective complexation of negatively charged siRNA. Active Ingredient caprylate complex were prepared and characterized successfully as reported in our earlier work because caprylate conjugates of Active Ingredient improve its lipophilicity, which in turn increase Active Ingredient loading into LPNs [33].

Box-Behnken design (State Ease) generated batches and the results of response variables (i.e., nanoparticle size and % entrapment efficiencies of Active Ingredient) are described in Table 1, and Figure 1 is a response surface plot of the combined effect of lipid and polymer concentrations at fixed molar ratio on particle size. Polymer concentration

Table 1. QbD-DoE Box-Behnken design for lipopolymeric nanoparticles.

| Independent variables | | | | Dependent variables | | |
|---|---|---|---|---|---|---|
| Run | Lipid concentration (mM) | Polymer concentration (mg/ml) | Lipid molar ratio† | Nanoparticle size (nM) | Entrapment efficiency (%) | Active Ingredient loading‡ (mg) |
| F1 | 5.00 | 0.67 | 1.50 | 194.2 ± 1.86 | 68.18 ± 3.21 | 7.25 |
| F2 | 1.00 | 0.50 | 2.75 | 142.1 ± 2.69 | 41.92 ± 2.67 | 3.77 |
| F3 | 3.00 | 0.67 | 2.75 | 156.5 ± 4.21 | 63.61 ± 1.69 | 6.12 |
| F4 | 1.00 | 0.67 | 4.00 | 136.2 ± 1.84 | 46.82 ± 2.80 | 3.94 |
| F5 | 3.00 | 0.83 | 1.50 | 164.6 ± 2.39 | 62.43 ± 1.83 | 6.08 |
| F6 | 3.00 | 0.83 | 4.00 | 144.7 ± 3.26 | 64.36 ± 2.78 | 6.18 |
| F7 | 5.00 | 0.50 | 2.75 | 174.1 ± 1.84 | 67.53 ± 2.56 | 6.24 |
| F8 | 3.00 | 0.50 | 1.50 | 169.5 ± 2.63 | 56.12 ± 1.89 | 5.12 |
| F9 | 1.00 | 0.83 | 2.75 | 136.9 ± 1.69 | 53.11 ± 3.21 | 4.68 |
| F10 | 1.00 | 0.67 | 1.50 | 144.7 ± 1.27 | 41.39 ± 2.69 | 3.78 |
| F11 | 5.00 | 0.67 | 4.00 | 169.2 ± 3.84 | 70.21 ± 2.93 | 7.26 |
| F12 | 3.00 | 0.50 | 4.00 | 149.3 ± 2.78 | 58.05 ± 1.11 | 5.20 |
| F13 | 3.00 | 0.67 | 2.75 | 157.9 ± 3.21 | 60.98 ± 3.83 | 5.81 |
| F14 | 3.00 | 0.67 | 2.75 | 151.5 ± 1.27 | 61.66 ± 2.17 | 5.86 |
| F15 | 5.00 | 0.83 | 2.75 | 173.7 ± 2.38 | 76.97 ± 1.48 | 8.29 |

†Lipid molar ratio: ratio of DPPC and cholesterol (DPPC: cholesterol: 3:2 = 1.50) where DOPE and DOTAP were kept constant in all formulations (e.g., for run F1, DPPC: cholesterol: DOPE: DOTAP – 3:2:1:1 at 5 mM total lipid concentration).

‡Active Ingredient loading: average values are reported. Values reported are mean ± standard deviation unless specified.

QbD-DoE: Quality by design–design of experiment.

had nonsignificant effect on nanoparticle size as seen from the reduced model (Equation 3). Furthermore, a higher PDI value was obtained at higher polymer concentration, indicating unfavorable distribution of hydrophilic and hydrophobic groups between polymers and lipids, which may progress into aggregate formation due to inadequate lipid coating. Zeta potential value on the lower side (~12 mV) was obtained with lower lipid concentration. Figure 1B shows the response surface plot of combined effect of lipid concentration and lipid molar ratio at constant polymer concentration on nanoparticle size. LPN size increased with increments in lipid concentration. Conversely, as the lipid molar ratio increased, nanoparticle size decreased. This might be due to lower cholesterol levels at the higher lipid molar ratio. Cholesterol is used to impart optimal fluidity and packing characteristics to the lipid bilayer [46]. Increasing the amount of cholesterol deteriorates LPN quality by disturbing bilayer packing, which in turn leads to wider polydispersity index values (PDI). At the optimal amount, phospholipid molecules align more strongly into the structure by filling empty spaces with cholesterol, and this will decrease the flexibility of the adjacent lipid chains. This interaction enhances the mechanical rigidity of lipid bilayers and lowers their lateral diffusion. In contrast, higher amounts of cholesterol to lipid bilayers disrupts local packing orders and increases the diffusion coefficient, which consequently leads to increase in PDI value [22,47].

The response surface plots (Figure 1D) shows the combined effect on entrapment efficiency of lipid and polymer concentrations at a constant molar ratio. It was concluded that increasing lipid and polymer concentrations would result in increments of entrapment efficiency (Equation 4). The increment in Active Ingredient caprylate entrapment efficiency could be due to the amphiphilic nature of block copolymer PEG-PLA in which PLA chains confer hydrophobicity to LPNs. Subsequetnly, Block copolymer can accommodate Active Ingredient caprylate within its matrix inside LPNs. The combination of lower lipid and higher polymeric content would lead to less drug entrapment due to inadequate lipid coating that, in addition, offers space for the drug in the bilayer compartment.

Reduced model equation in terms of coded factors

$$Y1\ \text{Nanoparticles size} = +155.30 + 18.91 * A - 9.20 * C - 4.13 * A * C \quad \text{(Eq. 3)}$$

$$\%\ \text{Entrapment efficiency} = +62.08 + 12.46 * A + 4.16 * B - 2.90 * A2 \quad \text{(Eq. 4)}$$

(A: Lipid concentration; B: Polymer concentration; C: Lipid molar ratio).

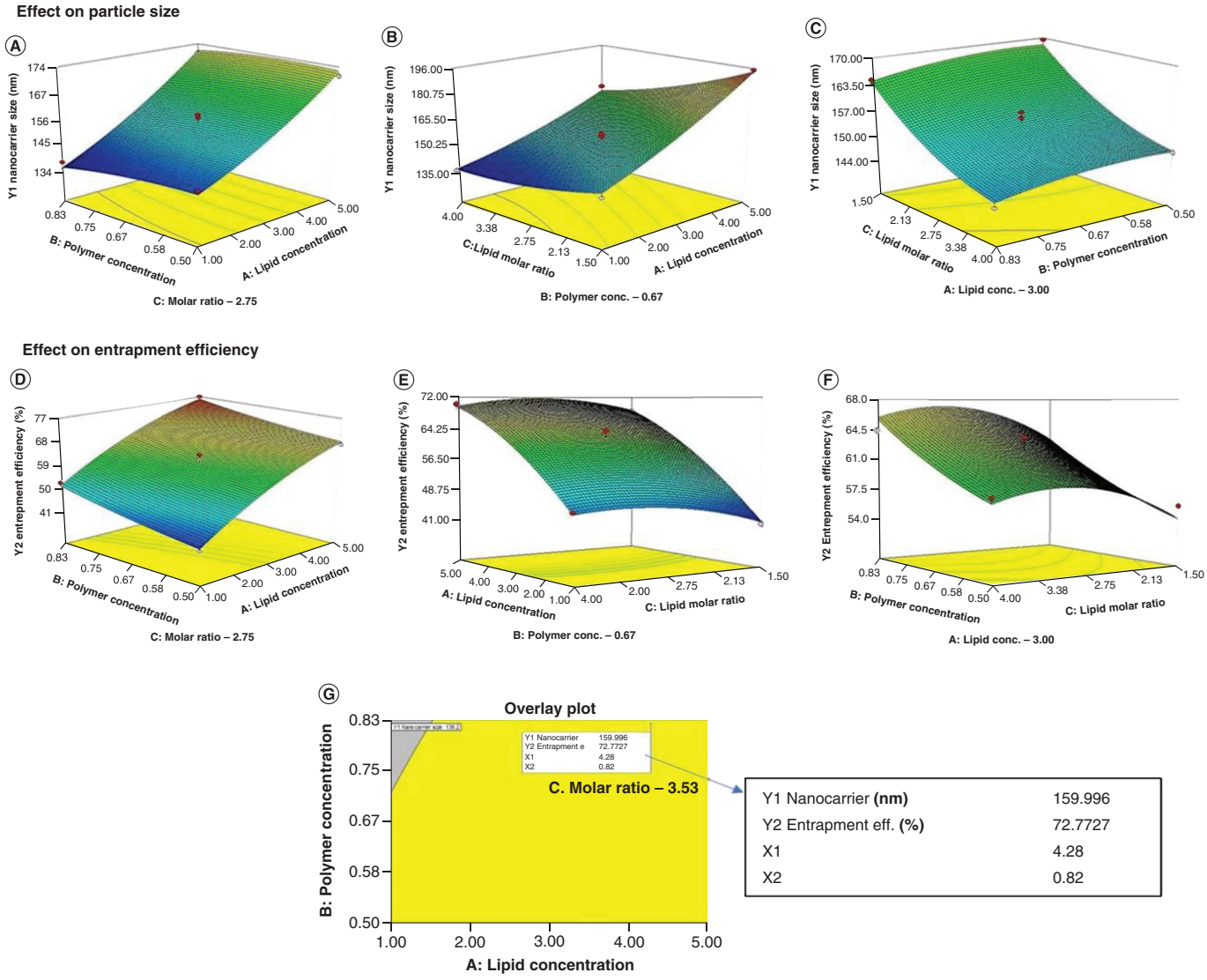


**Figure 1. Response surface plots for particle size and entrapment efficiency, respectively. (A & D)** Combined effect of lipid and polymer concentration. **(B & E)** Combined effect of lipid concentration and lipid molar ratio. **(C & F)** Combined effect of polymer concentration and lipid molar ratio. **(G)** Overlay plot.

**Table 2. Predicted responses for optimized batch.**

| Lipid conc. | Polymer concentration (mg/ml) | Lipid molar ratio | Size (nm) | Entrapment efficiency (%) | Desirability |
|---|---|---|---|---|---|
| 4.28 | 0.82 | 3.53 | 159.99 ± 3.45 | 72.77 ± 2.12 | 0.95 |
| QTPPL | | | 160 | Maximize | – |

QTPPL: Quality target product profile.
Data taken from [48].

Overlay plots (Figure 1G) were generated, and the results in Table 2 demonstrate the suitability of prediction by higher desirability value obtained for optimized formulation. The actual % entrapment efficiency of the optimized batch was found to be 71.53 ± 2.12%, and drug loading was found to be 0.29 mg per mg of total solid (lipid and polymer) content. In the present study, nanoparticle size was in the range of 155–165 nm (162.2 ± 3.45 nm) with a very good polydispersity index of 0.098. The zeta potential of LPNs was found to be +43.18 ± 1.83 mV, which is due to the presence of cationic lipid DOTAP. Positively charged particles will repel one other and provide

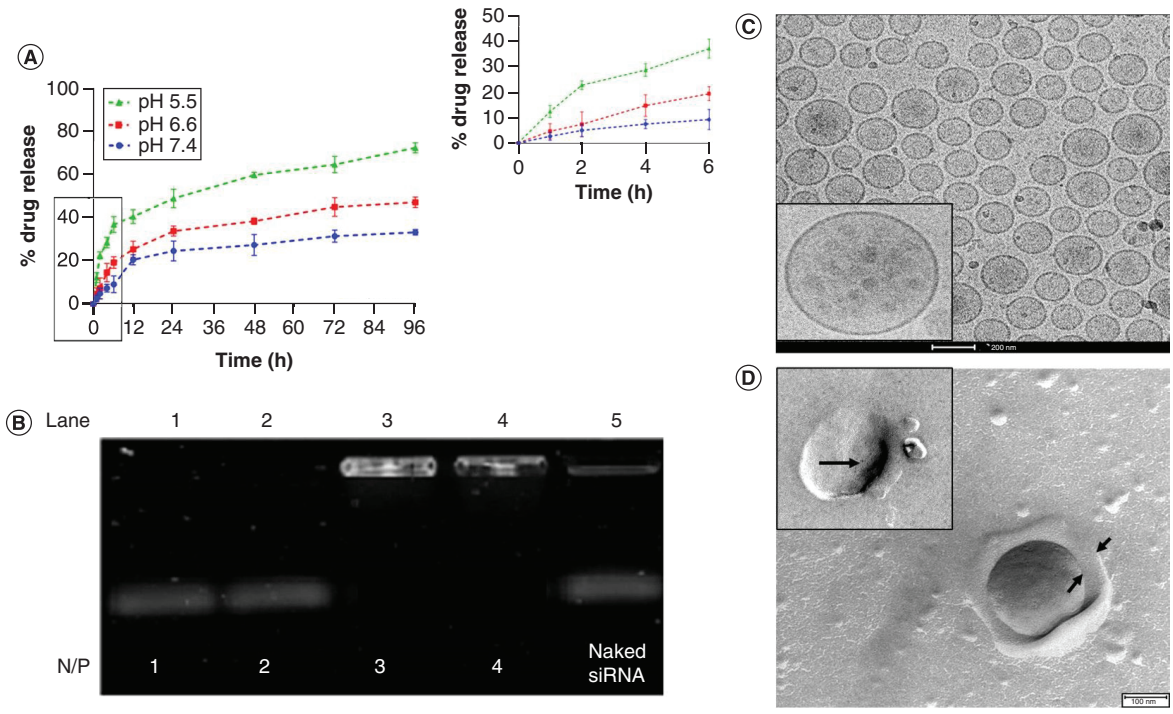


**Figure 2. Characterization of drug-loaded lipopolymeric nanoparticles. (A)** Active Ingredient caprylate release from PEGylated drug-loaded lipopolymeric nanoparticles (p-DLPNs) at different pH. **(B)** Gel retardation assay p-DLPNs and siRNA (p-SDLPNs) at different N/P ratios. **(C)** Cryo-TEM of p-SDLPNs. **(D)** Freeze fracture TEM for p-SDLPNs.
TEM: Transmission electron microscopy.

stability by preventing aggregation. Cationic charge is necessary for siRNA complexation and cellular uptake. The lipid estimation was carried out by Stewart's colorimetric method. This method relies on the ability of phospholipids to form a stable complex with ammonium ferrothiocyanate. The theoretical (calculated) amount of lipids in formulation was 4.9 ± 0.18 mg/ml, and amount of lipid found in LPNs by the Stewart method was 4.36 ± 1.38 mg/ml.

### *Drug release & kinetic study*

The drug release profile of DLPNs in various media is presented in Figure 2. At pH 7.4, a low amount of drug (~20%) was released within 12 h (Figure 2A). However, at pH 5.5, burst release was observed initially, with significant increments in release profile accounting to 41% release within first 12 h and ~73% at end of 96 h. It can thus be inferred that Active Ingredient caprylate release in the blood and normal tissues would be less thus leading to a low toxicity. The amount of drug released would be considerably higher inside pH 5.5 (i.e., lysosomes and endosomes of cancer cells). The release of Active Ingredient caprylate would depend on the drug encapsulated in the lipid bilayer and that entrapped in the polymeric core as well. Hence, drug release kinetics is governed by both lipid and polymer characteristics and the microenvironment of tissues and fluids. From the various kinetic model fitting (data not shown), it was concluded that for DLPNs, the best fit was the Higuchi model with $R^2$ value of 0.9844. This implies that the drug release would be a matrix diffusion-controlled release process, and drug encapsulated in the polymeric cores formed by PEG-PLA polymer would be released at a lower pH.

## Formulation & characterization of p-SDLPNs

### *Formulation of p-SDLPNs & siRNA complexation efficiency*

The charge-based interaction due to DOTAP's cationic charge in LPNs and anionic charge of siRNA was the driving force for siRNA complexation with DLPNs. Incubation time and temperature were optimized to ensure maximum complexation between siRNA and preformed LPNs. siRNA complexation was achieved (data not shown), with the maximum reached at an incubation time of 30 min and incubation temperature of 25°C. Below an N/P ratio of 3.0, a considerable amount of the siRNA traveled as free siRNA on agarose gel in the direction of the positive

Table 3. Characterization of PEGylated drug-loaded lipopolymeric nanoparticles with siRNA complexation.

| Batch | N/P ratio | siRNA complexation efficiency (%) | Effect of PEGylation on particle size | | Effect on siRNA complexation on zeta potential (mV) | |
|---|---|---|---|---|---|---|
| | | | Before PEGylation | After PEGylation‡ | Before complexation | After complexation |
| B1 | NA | NA | 132.2 ± 0.11 | 147.4 ± 1.79 | 38.16 ± 1.49 | 21.79 ± 0.79 |
| B2 | 1 | 34.78 ± 3.46 | 145.6 ± 0.86 | 160.5 ± 0.89 | 41.79 ± 0.67 | 25.93 ± 0.49 |
| B3 | 2 | 43.95 ± 4.18 | 128.2 ± 1.59 | 147.9 ± 0.16 | 48.37 ± 1.69 | 27.29 ± 1.73 |
| B4 | 3 | 95.83 ± 2.39 | 139.9 ± 0.45 | 153.2 ± 1.76 | 47.97 ± 0.49 | 25.39 ± 0.49 |
| B5 | 4 | 92.69 ± 2.76 | 132.2 ± 0.78 | 148.8 ± 0.79 | 53.61 ± 0.73 | 22.61 ± 1.79 |
| B6† | 3 | 90.36 ± 3.83 | 133.4 ± 1.59 | NA | 49.95 ± 1.49 | 36.56 ± 2.10 |

Batches B1– B6 have a similar formulation composition as shown in Table 2.
†Batch B6 was formulated without addition of DSPE PEG 2000.
‡With siRNA.
NA: Not applicable.
Data taken from [48].

electrode. This loose LPN complex may release siRNA before reaching the cell or may cause siRNA inactivation. However, maximum complexation was achieved at 3 and 4 N/P ratios as indicated by the visible band in the well itself, confirming absence of siRNA migration on agarose gel (Figure 2B). Thus, free siRNA was not present at N/P of 3 and 4, indicating maximum complexation of siRNA. Table 3 compares the siRNA complexation efficiency at different N/P ratios. The complexation efficiency of siRNA was ~35% at lower N/P ratio, whereas 90% complexation was achieved for N/P ratio of 3 and 4 (batch B4 and B5). Batch B4, with an N/P ratio of 3, was selected for subsequent experiments.

### *Size & zeta potential analysis*

The results of size changes due to PEGylation along with change in zeta potential due to siRNA complexation are presented in Table 3. The postinsertion method of PEGylation considerably increased the particle size for batches B1–B5, perhaps because of hydration volume increments on the surface. Moreover, size also depended on the PEG-lipid chain length [49]. The spontaneous process of the addition of DSPE PEG-2000 into preformed LPNs is governed by the hydrophobic interactions of lipids and hydrophobic end of lipopolymeric nanoparticles [10]. Zeta potential was considerably decreased after siRNA complexation, and surface interaction between negatively charged siRNA and positively charged LPNs was observed [50,51]. As evident from the zeta potential value of batch B6 (non-PEGylated batch with siRNA complexation), which decreased from ~50 mV to 36 mV, the values in batches B1–B5 decreased to a greater extent. This suggests that the PEGylation layer not only takes part in increasing the size/hydrodynamic radii of the carrier but could also be affecting the overall charge distribution and be partly shielding the charge on the LPNs. This effect has been well reported in the literature [52,53].

### *Cryo & freeze fracture TEM*

Confirmation of LPN structure was made by cryo-TEM, which demonstrated unilamellarity in structure and had a particle size <200 nm. The configuration of PEG-PLA matrix core in LPNs was also established through the freeze fracture microscopy image, wherein it can be seen as dense area surrounded by the lipid outer membrane. It also revealed solid polymeric matrix core inside LPNs (Figure 2C).

## Development of DPI of p-SDLPNs

### *Preparation of p-SDLPNs-DPI*

The LPN formulation characteristic should not be altered to a significant extent, which would affect the performance of the product after lyophilization. To evaluate the changes, particle size, PDI, zeta potential and physical appearance of the product were evaluated after lyophilization. Although all the cryoprotectants were successfully lyophilized to yield dry cake, there were differences in the physical appearance of it. The cake from lactose showed shrinkage. The reconstitution behavior for the lactose-containing formulation (in water) was poor, and there was a higher moisture content in the lyophilized cake (2–4% w/w). The cake formed by trehalose were more homogenous and porous in nature. Therefore, it can be inferred that trehalose would require minimal postprocessing and had a good product appearance. The size ($D_{50}$) of the obtained lyophilized powder containing nanoparticles was 18.62 µm using the Malvern master sizer. D10 and D90 values were 1.18 and 51.97 µm, respectively. Reconstitution of

Table 4. Solid-state characterization of p-SDLPNs–dry powder inhalant formulations.

| Formulation† to carrier mass ratio (w/w) | Tapped density (g/cc) | Angle of repose (°) | Carr's index | Moisture content (% w/w) |
|---|---|---|---|---|
| 1:0 | 0.8 ± 0.04 | 41.68 ± 1.48 | 34.78 ± 2.78 | 1.60 ± 0.30 |
| **Inhalac 230** | | | | |
| 1:1 | 0.67 ± 0.07 | 37.94 ± 2.93 | 38.93 ± 3.84 | 1.41 ± 0.28 |
| 1:3 | 0.59 ± 0.11 | 29.78 ± 1.48 | 22.89 ± 1.69 | 1.59 ± 0.31 |
| 1:5 | 0.58 ± 0.05 | 28.54 ± 0.98 | 21.20 ± 1.45 | 1.60 ± 0.25 |
| **Respitose SV003** | | | | |
| 1:1 | 0.63 ± 0.02 | 32.48 ± 3.28 | 19.68 ± 3.28 | 1.59 ± 0.30 |
| 1:3 | 0.41 ± 0.04 | 22.84 ± 1.94 | 15.93 ± 2.75 | 1.85 ± 0.27 |
| 1:5 | 0.40 ± 0.02 | 20.61 ± 1.50 | 15.11 ± 1.93 | 1.70 ± 0.39 |

†PEGylated drug-loaded lipopolymeric nanoparticles with siRNA complexation (p-SDLPNs) lyophilized formulation with trehalose as cryoprotectant (LPNs:cryoprotectant ratio: 1:6 w/w). Values are mean ± standard deviation.

lyophilized formulation yielded LPNs of 160.5 nm, which is near the size of LPNs before lyophilization. The zeta potential values were unaffected after reconstitution. Lyophilized formulation containing trehalose showed <2% w/w moisture content; thus it was selected for further processing [54]. To prepare the DPI, the lyophilized product was mixed with two grades of lactose as carrier. Solid-state characterizations, such as tapped density, Carr's compressibility index and angle of repose, were measured for both mixtures and is reported in Table 4. As can be seen, at mass ratio of 1:1 for both the carriers, the powder characteristics were inadequate to achieve excellent flow properties. As the carrier mass ratio was increase there was improvement in flow properties, which was evident due to the increase in amount of carrier compared to the formulation amount. However, at equal mass ratio, among the two carrier, Respitose displayed superior performance. Furthermore, between 1:3 and 1:5, the quantum of improvement in flow properties was nonsignificant.

### *In vitro deposition studies using the Anderson cascade impactor*

From the foregoing powder characterization, although Respitose provided better results in terms of flow properties; nonetheless, it is important to evaluate the behavior after aerosolization because, despite having good flow properties, separation of carrier from the substrate (LPNs) is required to achieve deposition of formulation at the target site in the lungs. The interaction forces between carrier and the substrate should thus be optimal to provide effective aerosolization as well as carrier separation. Thus, both carriers were evaluated for deposition studies. The respirable fraction or FPF is defined as particle mass below size 5 µm. Aerodynamically light porous particles would lead to enhanced FPF. In the current study, the target was set to develop aerodynamically light porous particles having high emitted dose and MMAD of particles between 1 and 3 µm to obtain higher FPF and avoidance of natural clearance mechanism in lungs through alveolar macrophage uptake. The lyophilized formulation powder was mixed separately with Respitose SV003 and Inhalac 230 at different weight ratios, as shown in Table 5. The mixing was performed by the alligation method at low relative humidity. The powder mass was then filled into hard gelatin capsules (size 3) and stored in HDPE bottles containing silica bags as desiccant.

The data revealed the important role of coarse carriers in the development of the DPI. As shown in Table 5, there was a low emitted dose (i.e., 31.35%) at lower carrier mass ratios. It was inferred that bulk properties were dominated by lyophilized bulk with sticky/cohesive nature with poor fluidization. The addition of a coarse carrier at a higher mass ratio led to improvement in emitted dose up to 76.61 and 79.82% for Inhalac 230 and Respitose SV003, respectively, due to improved fluidity. However, the FPF and MMAD observation revealed differences in inter-particulate forces while using two different carriers. Respitose SV003 showed higher FPF than the Inhalac 230 i.e. 40.56% and 31.95%, respectively, at carrier mass ratio of 1:5. Thus, Respitose SV003 was selected as the carrier for this DPI formulation; because there was little difference in aerodynamic behavior between the 1:3 and 1:5 mass ratios, the 1:3 ratio was chosen [55]. It was observed that optimized carrier concentration is necessary to achieve detachment of LPNs from the carrier molecule, leading to higher FPF. This promising aerosolization performance led to fabrication of aerodynamic light DPI particles having good flow properties, low density and lower moisture content. The theoretical aerodynamic diameter of any inhalational nanoparticles must lie within range of 1 to 5 µm for deep lung deposition. Particles with an aerodynamic diameter <1 µm are exhaled, and particles >5 µm are

Table 5. Aerodynamic behavior of p-SDLPNs with carriers at different weight ratios.

| Formulation† to carrier mass ratio (w/w) | Recovered dose (%) | Emitted dose (%) | MMAD (μm) | FPF (%) | GSD |
|---|---|---|---|---|---|
| 1:0 | 50.05 ± 1.85 | 31.35 ± 3.72 | 7.16 ± 0.28 | 8.51 ± 0.13 | 4.5 |
| Inhalac 230 | | | | | |
| 1:1 | 88.20 ± 2.74 | 66.42 ± 1.69 | 6.96 ± 0.93 | 11.02 ± 1.451 | 3.5 |
| 1:3 | 94.13 ± 1.94 | 75.13 ± 3.27 | 5.33 ± 0.57 | 27.87 ± 3.17 | 2.8 |
| 1:5 | 93.60 ± 2.05 | 76.61 ± 2.56 | 4.62 ± 0.55 | 31.95 ± 3.10 | 2.5 |
| Respitose SV003 | | | | | |
| 1:1 | 90.09 ± 1.49 | 62.46 ± 2.73 | 6.30 ± 0.26 | 18.41 ± 4.28 | 3.7 |
| 1:3 | 93.14 ± 3.17 | 78.91 ± 1.38 | 3.34 ± 0.27 | 37.48 ± 5.86 | 2.2 |
| 1:5 | 95.15 ± 1.28 | 79.82 ± 2.15 | 3.30 ± 0.30 | 40.56 ± 3.90 | 2.1 |

†p-SDLPNs lyophilized formulation with trehalose as cryoprotectant (LPNs to cryoprotectant ratio: 1:6 w/w). Values are mean ± standard deviation.
FPF: Fine powder fraction; GSD: Geometric standard deviation; MMAD: Mass median aerodynamic diameter; p-SDLNP: PEGylated drug-loaded lipopolymeric nanoparticles with siRNA complexation.

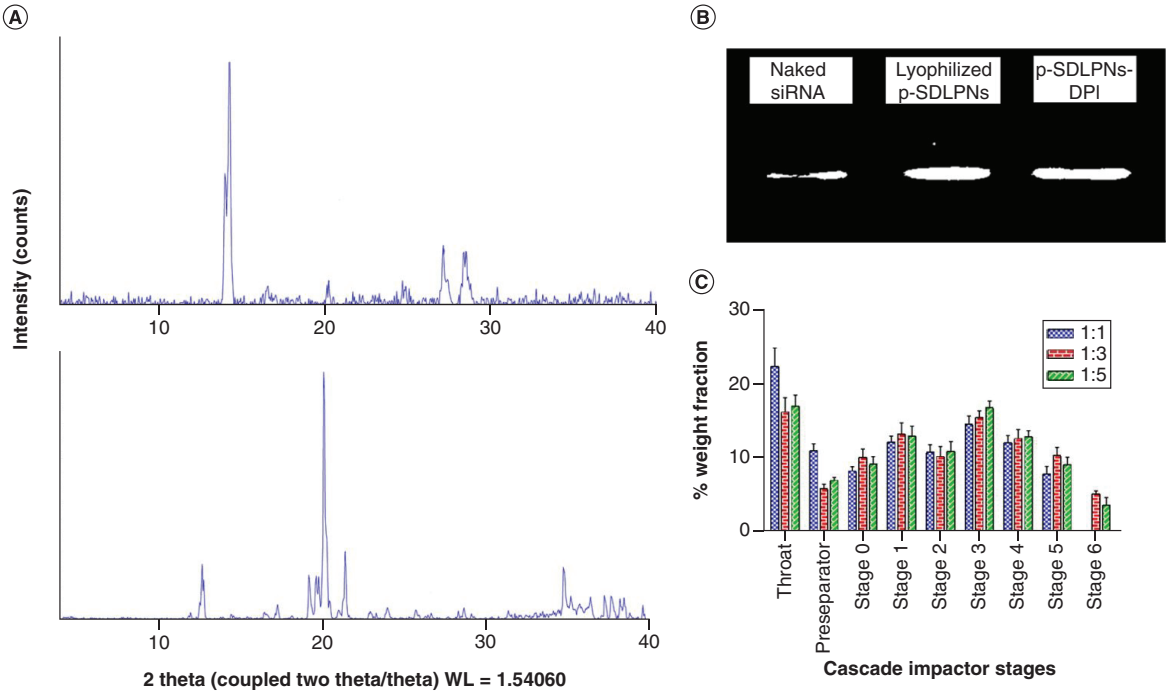


**Figure 3. Charecterization of p-SDLPNs. (A)** Powder x-ray diffraction of Active Ingredient and PEGylated drug-loaded lipopolymeric nanoparticles with siRNA complexation (p-SDLPNs-DPI). **(B)** Integrity of siRNA after dry powder inhalant formation. **(C)** *In vitro* pulmonary deposition pattern (using cascade impactor) of p-SDLPNs using Respitose SV003 (legends indicates formulation: carrier mass ratio).

predominantly deposited in larger airways (i.e., mouth and throat). The powder processing leads to enhancement of powder characteristics, such as cohesive–adhesive interactions, flow properties and fluidization of the lyophilized bulk. Addition of the optimal amount of fine carrier particles occupies the high-energy active sites on the surface of coarse particles of lyophilized LPNs, thereby avoiding strong adherence of DLPN particles to lyophilized coarse particles of cryoprotectant. The carrier forms a loose reversible bond with lyophilized LPN particles, resulting into a higher FPF [56].

### *Powder x-ray diffraction*

Powder x-ray diffraction data (Figure 3A) revealed that DPI formulation retained the crystalline nature of the bulk drug, which stabilizes the formulation against hygroscopicity during the drying stage of lyophilization. The

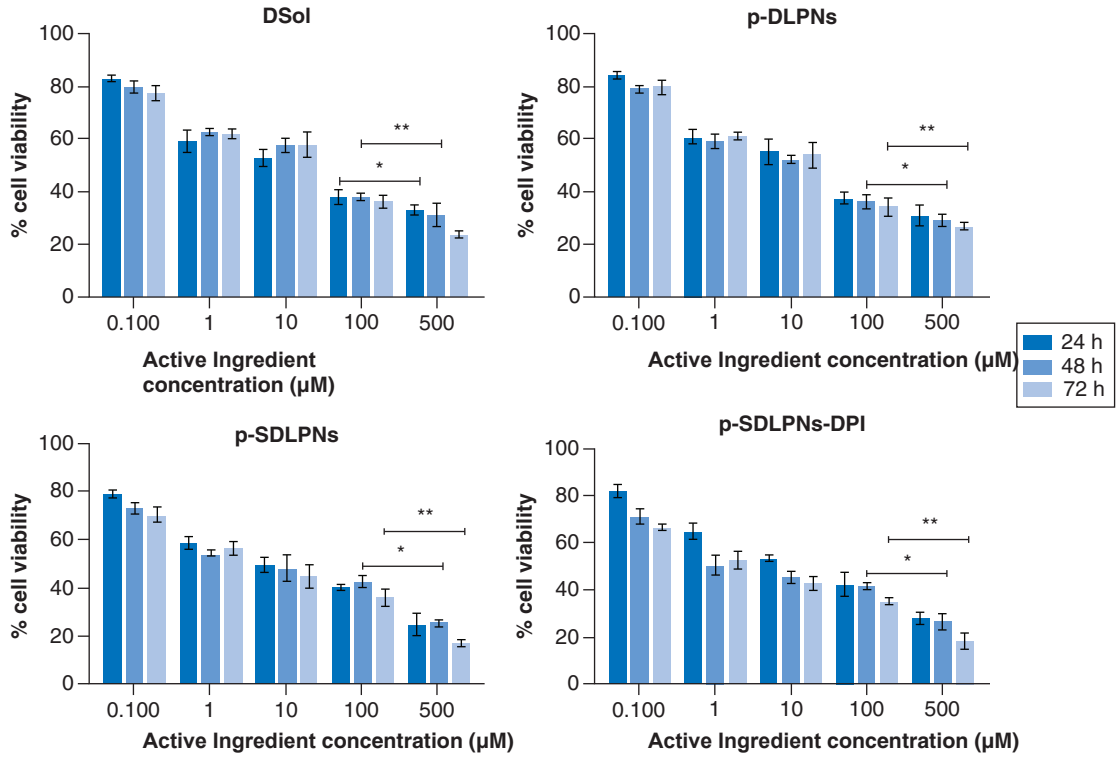


**Figure 4. Cytotoxicity studies. (A)** Cytotoxicity of DSol. **(B)** Cytotoxicity of PEGylated drug-loaded lipopolymeric nanoparticles (p-DLPNs). **(C)** Cytotoxicity of p-DLPNs with siRNA (p-SDLPNs). **(D)** Cytotoxicity of p-SDLPNs with dry power inhalant (DPI).

retention of this crystalline structure is of significant importance because changes during lyophilization would affect the bonding behavior between LNPs and the carrier. The presence of crystallinity is suitable for particle agglomeration and adsorption onto the surface of carrier materials instead of forming stronger hydrogen bonding. Herein, the cryoprotectant serves as a barrier preventing the aggregation of LNPs in accordance with particle isolation hypothesis and also indicates the maintenance of LNPs size and transfection efficiency [57]. Conversion to amorphous form leads to higher surface adhesion energy than crystalline forms, which leads to poor deaggregation after fluidization in the air stream. In contrast, crystalline forces are weak and easily overcome by the turbulent shear produced during inspiration. The crystallinity is also helpful for better shelf stability during shelf storage due to low hygroscopicity.

### *Integrity of siRNA*

After inhalation, the formulation made contact with mucosal membranes with nucleases. Mucosal nuclease can degrade and deactivate siRNA, and such siRNA inactivation would result into lack of efficacy and therapeutic failure inside the cells at the site. Therefore, it was essential to confirm that the siRNA was intact in the p-SDLPNs-DPI formulation. From results of band density (Figure 3B) obtained by gel electrophoresis, it can be concluded that the DPI formulations retained the integrity of the siRNA even after lyophilization and powder processing. siRNA complexation was found to be 97.32 ± 2.79% before lyophilization and changed to 95.82 ± 2.21% and 94.21 ± 1.58% after lyophilization and powder processing to formulate DPI, respectively.

## *In vitro* cell line study

### *Cytotoxicity studies by MTT assay*

Figure 4A–D & Table 6 provide MTT results and $IC_{50}$ values, respectively. At the maximum concentration used for testing, only 10% cell death was observed for blank LPNs, indicating the carrier was noncytotoxic (data not presented). Similar cytotoxicity at different concentrations and times was demonstrated by Dsol and p-DLPNs, and fold change in $IC_{50}$ of the latter with respect to the former were only 1.04, 1.18 and 1.03 at 24, 48 and 72 h,

Table 6. $IC_{50}$ values.

| Formulation | $IC_{50}$ (μM) | | |
|---|---|---|---|
| | 24 h | 48 h | 72 h |
| Dsol | 14.92 | 13.18 | 11.11 |
| p-DLPNs | 14.41 | 11.20 | 10.79 |
| p-SDLPNs | 9.48 | 5.81 | 3.32 |
| p-SDLPNs-DPI† | 10.01 | 6.16 | 3.95 |

†Nonsignificant changes ($p < 0.05$) compared to p-SDLPNs.
Three independent replicates of experiments were performed.
p-DLPN: PEGylated drug-loaded lipopolymeric nanoparticle; p-SDLPN: p-DLPN with siRNA; p-SDLPN-DPI: p-SDLPN with dry powder inhalant.

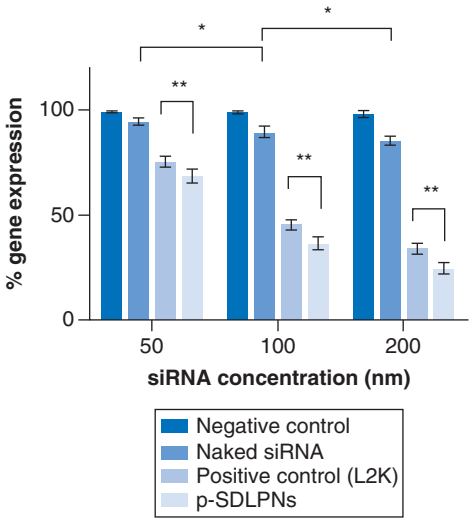


Figure 5. Gene expression study by real-time PCR for negative control (scrambled siRNA), naked siRNA, transfection standard (L2K) and coloaded formulation (PEGylated drug-loaded lipopolymeric nanoparticles with siRNA [p-SDLPNs]).
**$p < 0.01$.

respectively, which suggests that an equivalent concentration of drug could have been presented to the cells. This nonsignificant improvement in cytotoxic potential can be attributed to the slow drug release from the formulation due to sustained release, and this is consistent with the results reported in other studies [58,59]. The most noteworthy impact on the cell viability profile was observed with p-SDLPNs and p-SDLPNs-DPI (redispersed) formulation, wherein a 3.35- and 2.81-fold improvement in $IC_{50}$ value was obtained at 72 h. This decline in value may be due to the impact of siRNA on the drug efflux inhibition. At 24 and 48 h, the fold decline in values was 1.57 and 2.27, respectively, for p-SDLPNs, whereas it was 1.49- and 2.13-fold for redispersed LPNs. These valued indicated that redispersed LPNs have similar effect as that of p-SDLPNs formulation. A549 effluxes various chemotherapeutic agents from the cells, and Active Ingredient is one of these, due to presence of ABC efflux pump on the cells [35]. Thus, the approach of codelivering siRNA with the drug provided synergistic effects and led to enhanced cidal activity [60].

### *Gene knock-down by RT-PCR*

For gene/drug or combination therapeutics to exhibit therapeutic effect, it is necessary for the carrier to efficiently transfect the cells and release the payload, retreat from endosomes and release nascent siRNA/DNA in the cytoplasmic or nuclear compartment. On the basis of the studies just described, the optimized formulation (p-SDLPNs) with different levels of siRNA were subjected to RT-PCR to assess expression against control cells. The gene expression level was not inhibited by negative control siRNA (NC-siRNA), thus confirming the specificity of siRNA sequence. For the treatment groups, a concentration-dependent inhibition of gene expression was noted (Figure 5). A low degree of reduced mRNA expression was affected by naked siRNA, whereas for L2K, at the highest concentration tested, a knockdown efficiency of 66% was observed. Transfection of cells with 100 and 200 nM siRNA containing LPNs strongly downregulated the ABCC3 levels with % gene expression of 37 and 25%, respectively. For 50 nM, the level of downregulation was only 30%. However, LPNs containing 100 nM siRNA and above suppressed more than 65% of *ABCC3* gene expression. Further evidence of nanoparticulate formulation internalization was estimated in our previous work, and results demonstrated significant increment

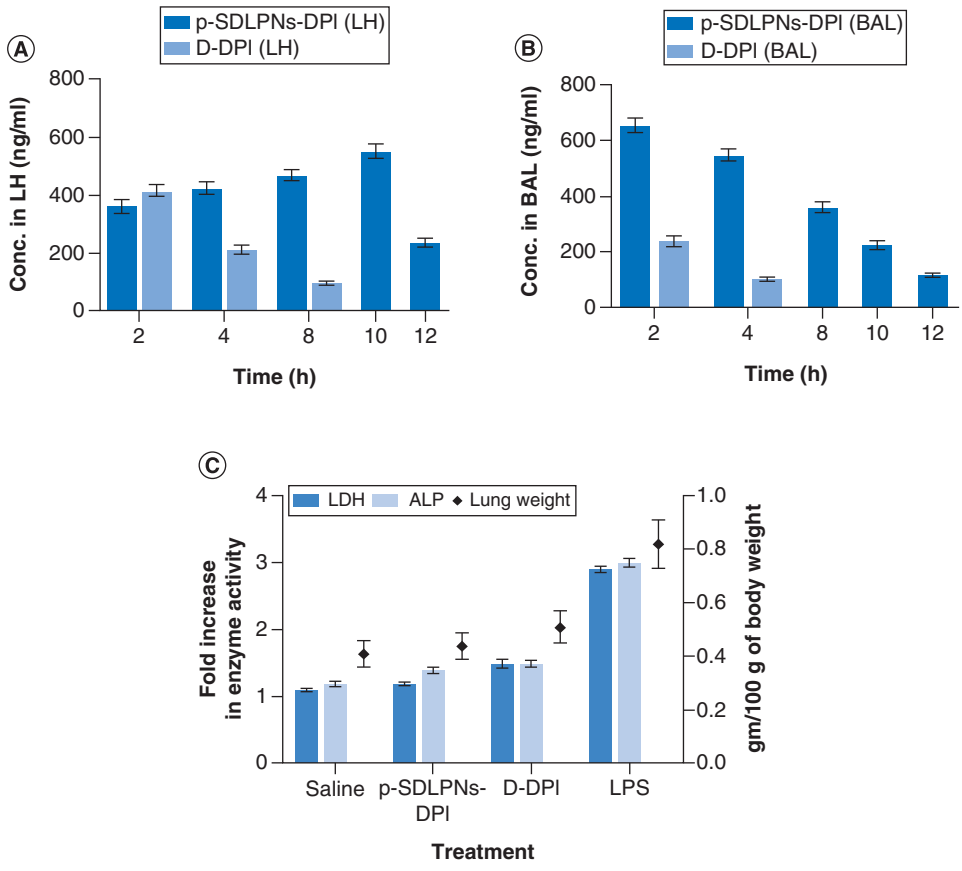


**Figure 6.** **Active Ingredient concentration in (A) lung homogenate [19] and (B) BAL at different time intervals. (C)** Enzyme activity and L/B ratio.
BAL: Bronchoalveolar lavage; L/B: Lung weight/body weight.

in fluorescence intensity of formulation compared to naked siRNA, indicating higher transfection efficiency. It was thus concluded that the formulated LPNs effectively transfected the cells and delivered the payload into the cells [30].

## *In vivo* studies

### *Pulmonary pharmacokinetic*

*In vivo* evaluation was carried out by assessing the concentration of drug in BAL and LH after the administration of p-SDLPNs-DPI and of plain drug (D) as DPI (D-DPI: plain drug [Active Ingredient] DPI) (Figure 6A & B). The dose equivalent to 200 µg was given intratracheally. Drug quantity present in the LH was noted because the drug absorbed and accessible for the pharmacological response and the drug quantity present in the BAL were taken as drug not absorbed into the lung tissue but still retained in the bronchial spaces (in LPN encapsulated form). The later represents a drug reservoir that ultimately would be absorbed by the lung tissue. The mass balance of Active Ingredient between the drug absorbed (drug in LH) and drug entrapped within LPNs (drug in BAL) was near to 95% [40].

The pulmonary pharmacokinetic parameters were calculated and are depicted in Table 7. A $t_{\frac{1}{2}}$ value of 8.06 h was obtained with p-SDLPNs-DPI compared with 2.20 h with DPI of Active Ingredient drug (D-DPI). There was an improvement in AUC for LPNs compared with the AUC of drug. LPNs showed 2.44 times higher AUC values than that of drug. MRT of p-SDLPNs-DPI for also increased 2.5-fold. It can be inferred from the above trend that plain Active Ingredient would either get quickly absorbed into the systemic circulation from the lungs or get quickly metabolized whereas p-SDLPNs-DPI showed significantly higher residence time in lungs.

Table 7. Pulmonary Pharmacokinetic Parameters after intratracheal instillation.

| Formulation | $AUC_{total}$ (ng.h/ml) | $C_{max}$ (ng/ml) | $T_{max}$ (h) | $t_{1/2}$ (h) | MRT (h) |
|---|---|---|---|---|---|
| D-DPI | 4619 ± 121.79 | 652 ± 5.69 | 2 ± 0.05 | 2.20 ± 0.1 | 4.40 ± 0.16 |
| p-SDLPNs-DPI | 11314 ± 95.38 | 1061 ± 9.27 | 12 ± 0.1 | 8.06 ± 0.16 | 11.41 ± 0.07 |

Values expressed as mean ± SD (where n = 6).
AUC: Area under the curve; D-DPI: Dry powder inhalant with Active Ingredient; MRT: Mean residence time; p-SDLPNs-DPI: PEGylated drug-loaded lipopolymeric nanoparticles with siRNA in dry powder inhalant.

### *Enzymatic activity estimation*

A graph of the LDH and ALP enzyme activities and L/B (lung weight/body weight) ratio is shown in Figure 6C. The weight of the lungs was normalized to 100 g of body weight for comparison purposes. L/B ratios were obtained 0.41 for the saline-treated animals, whereas for lipopolysaccharides, it was 0.80 due to accumulation of extracellular fluids in mucosa of respiratory cell, indicating edema and lung cell injury. L/B ratio was lowest for the p-SDLPNs-DPI formulation, suggesting efficacious activity against cancer cells. Activities of LDH and ALP were highest in lipopolysaccharides (positive control), and p-SDLPNs-DPI exhibited similar activity compared with saline control, which indicated a favorable safety profile for the DPI formulation. The elevated levels of LDH and ALP enzymes in BAL fluid are one of the biochemical indicators to evaluate lung cell injury. The pattern of change of isoenzymes can be used for diagnosis [61].

## Conclusion

In the current investigation, hybrid nanocarriers were developed for combined delivery of Active Ingredient and siRNA through the pulmonary route. Using response surface methodology, we investigated the impact of varying lipid and polymer concentrations in a formulation of the hybrid system, and it can be concluded that amphiphilic drug encapsulation could be improved by incorporating block copolymers in the formulation. Because our strategy was to complex siRNA by a charge-based interaction onto the nanocarrier, it was important to carefully design the incorporation of cationic lipids to confer an overall positive charge to the formulation for effective complexation. The lyophilized formulation intended for pulmonary delivery should retain its crystalline nature for effective aerosolization and to achieve greater deposition in the airway. We observed an approximately threefold improvement in $IC_{50}$ value due to drug efflux inhibition mediated by siRNA, which points to the importance of evaluating synergistic therapeutic agent-based approaches for maximizing efficacy in drug resistance. Delivery of ABCC3 siRNA grafted onto LPNs against ABCC3 protein exerted a significant gene knockdown effect, followed by sensitization of cancer cells. Formulated p-SDLPNs-DPI successfully delivered the siRNA and Active Ingredient caprylate directly into the lung. The core idea of masking resistance to chemotherapy in lung cancer was thus fulfilled.

## Future perspective

Combination therapy for cancer has evolved exponentially in the past 2 decades; among these, some gene-therapy-based products are in clinical trials, and a few have been approved. With US FDA approval of the first-ever siRNA product Onpattro (patisiran) for the transthyretin-mediated amyloidosis in adult patients, delivery of siRNA can be seen as the future of gene-based therapy. The current research can provide a platform for such strategies in which a combinatorial approach can be used for sensitizing cells to chemotherapy. It also establishes the use of a 3D cell culture model to bridge the gap between 2D cell cultures and animal models. This could transform the future of the gene targeting in cancer treatment from universal chemotherapy to a personalized treatment based on the patient's genomic profile and immune status, the mechanism of the resistance and gene-related malignancies. The developed system is expected to be less toxic due to the loading of genes to nonviral carriers and will possess high cure rates compared with currently available treatment approach.

### Acknowledgments

The acknowledge the contribution by following: Prof Paola Luciani and her research group (Former Professor of Institute of Pharmacy, Friedrich schiller university of Jena, Germany) for providing laboratory and technical support; Department of Science and Technology (DST), Government of India and German academic exchange service (DAAD) for financial assistance for this collaborative project between Faculty of Pharmacy, The Maharaja Sayajirao University of Baroda and Friedrich schiller university of Jena, Germany; Dr Bhavin A Vyas of Maliba Pharmacy College for animal studies; & Central salt and marine chemicals research institute (CSMCRI), Bhavnagar for Cryo-TEM & SEM studies. All animal experiments and protocol described in the present study were

approved by the Institutional Animal Ethical Committee (IAEC) of Maliba Pharmacy College, Uka Tarsadia University, Bardoli wide protocol MPC/IAEC/02/2019 and with permission from committee for the purpose of control and supervision of experiments on Animals (CPCSEA), Ministry of Social Justice and Empowerment, Government of India.

### Financial & competing interests disclosure

The authors have no relevant affiliations or financial involvement with any organization or entity with a financial interest in or financial conflict with the subject matter or materials discussed in the manuscript. This includes employment, consultancies, honoraria, stock ownership or options, expert testimony, grants or patents received or pending, or royalties.

No writing assistance was utilized in the production of this manuscript.

### Ethical conduct of research

The authors state that they have obtained appropriate institutional review board approval or have followed the principles outlined in the Declaration of Helsinki for all human or animal experimental investigations. In addition, for investigations involving human subjects, informed consent has been obtained from the participants involved.

### Summary points

- The formulation of a dry powder for pulmonary delivery of lipopolymeric nanoparticles (LPNs) consisting of drug and siRNA for multidrug-resistant lung cancer was studied.
- Optimization of LPN formulation was undertaken using the quality by design–design of experiment approach.
- Aerodynamic properties of dry powder for inhalation (DPI) for lung delivery was optimized.
- There was an up to threefold reduction in $IC_{50}$ values for the DPI formulation compared with the drug solution dosage form and an improvement in area under the curve and mean residence time of Active Ingredient in the lung with inhaled delivery.
- Silencing of multidrug-resistant gene ABCC3 (MRP3) through custom screened siRNA provided synergistic therapeutic activity by decreasing the resistance of cells to a chemotherapeutic agent such as Active Ingredient.

## References

Papers of special note have been highlighted as: • of interest; •• of considerable interest


1. Torre LA, Siegel RL, Jemal A. Lung cancer statistics. In: *Lung Cancer and Personalized Medicine.* Ahmad A, Gadgeel S (Eds). Springer, NY, USA, 1–19 (2016).
2. Creixell M, Peppas NA. Co-delivery of siRNA and therapeutic agents using nanocarriers to overcome cancer resistance. *Nano Today* 7(4), 367–379 (2012).

• **Advantages of combinatorial approach in lung cancer are detailed in this paper.**

3. Peters GJ. Cancer drug resistance: a new perspective. *Cancer Drug Resist.* 1, 1–5 (2018).
4. Patel NR, Pattni BS, Abouzeid AH, Torchilin VP. Nanopreparations to overcome multidrug resistance in cancer. *Adv. Drug Deliv. Rev.* 65(13–14), 1748–1762 (2013).

•• **The role of nanocarriers for overcoming drug resistance in cancer is evaluated.**

5. Hu B, Zhong L, Weng Y *et al.* Therapeutic siRNA: state of the art. *Signal. Transduct. Target. Ther.* 5(1), 1–25 (2020).
6. Szakács G, Paterson JK, Ludwig JA *et al.* Targeting multidrug resistance in cancer. *Nat. Rev. Drug Discov.* 5(3), 219–234 (2006).

•• **Different targets on the tumor cell surface are identified and their use for the drug targeting is described.**

7. Tian Z, Liang G, Cui K *et al.* Insight into the prospects for RNAi therapy of cancer. *Front. in Pharmacol.* 12, 308 (2021).
8. Chalbatani GM, Dana H, Gharagouzloo E *et al.* Small interfering RNAs (siRNAs) in cancer therapy: a nano-based approach. *Int. J. Nanomed.* 14, 3111–3128 (2019).
9. Cao F, Wan C, Xie L *et al.* Localized RNA interference therapy to eliminate residual lung cancer after incomplete microwave ablation. *Thorac. Cancer* 10(6), 1369–1377 (2019).
10. Saad M, Garbuzenko OB, Minko T. Co-delivery of siRNA and an anticancer drug for treatment of multidrug-resistant cancer. *Nanomedicine (Lond).* 3(6), 761–776 (2008).
11. Kandil R, Merkel OM. Pulmonary delivery of siRNA as a novel treatment for lung diseases. *Ther. Deliv.* 10(4), 203–206 (2019).
12. Das M, Musetti S, Huang L. RNA interference-based cancer drugs: the roadblocks, and the 'delivery' of the promise. *Nucleic Acid Ther.* 29(2), 61–66 (2019).
13. Adjei A. *Inhalation Delivery of Therapeutic Peptides and Proteins.* Adjei A (Ed). CRC Press, FL, USA (1997).
14. Islam N, Gladki E. Dry powder inhalers (DPIs) – a review of device reliability and innovation. *Int. J. Pharm.* 360(1–2), 1–11 (2008).

•• **Development of a dry powder inhalant for targeted pulmonary delivery of nanocarriers is described. The crucial role played by device and powder characteristics in pulmonary delivery is discussed.**

15. Kasper JC. Lyophilization of nucleic acid nanoparticles [Doctoral thesis]. https://edoc.ub.uni-muenchen.de/14425/1/Kasper_Julia_Christina.pdf

16. Pfeifer C, Hasenpusch G, Uezguen S *et al.* Dry powder aerosols of polyethylenimine (PEI)-based gene vectors mediate efficient gene delivery to the lung. *J. Control. Release.* 154(1), 69–76 (2011).

17. Telko MJ, Hickey AJ. Dry powder inhaler formulation. *Respir. Care* 50(9), 1209–1227 (2005).

• **Formulation characteristics of dry powders for effective pulmonary targeting.**

18. Mangal S, Gao W, Li T, Zhou QT. Pulmonary delivery of nanoparticle chemotherapy for the treatment of lung cancers: challenges and opportunities. *Acta Pharmacol. Sin.* 38(6), 782–797 (2017).

19. Carvalho TC, Carvalho SR, Mcconville JT. Formulations for pulmonary administration of anticancer agents to treat lung malignancies. *J. Aerosol. Med. Pulm. Drug. Deliv.* 24(2), 61–80 (2011).

20. Jensen DK, Jensen LB, Koocheki S *et al.* Design of an inhalable dry powder formulation of DOTAP-modified PLGA nanoparticles loaded with siRNA. *J. Control Release.* 157(1), 141–148 (2012).

21. Rosière R, Berghmans T, De Vuyst P *et al.* The position of inhaled chemotherapy in the care of patients with lung tumors: clinical feasibility and indications according to recent pharmaceutical progresses. *Cancers* 11(3), 329 (2019).

22. Akbarzadeh A, Rezaei-Sadabady R, Davaran S *et al.* Liposome: classification, preparation, and applications. *Nanoscale Res. Lett.* 8(1), 102 (2013).

23. Gautschi O, Mack PC, Heighway J, *et al.* Molecular biology of lung cancer as the basis for targeted therapy. In: *Lung Cancer.* Pandya KJ, Brahmer JR, Hidalgo M (Eds). CRC Press, FL, USA, 11–34 (2016).

24. Hadinoto K, Sundaresan A, Cheow WS. Lipid–polymer hybrid nanoparticles as a new generation therapeutic delivery platform: a review. *Eur. J. Pharm. Biopharm.* 85(3), 427–443 (2013).

•• **The role of nanocarriers as a therapeutic delivery platform for various diseases is discussed.**

25. Zamboni WC, Torchilin V, Patri AK *et al.* Best practices in cancer nanotechnology: perspective from NCI nanotechnology alliance. *Clin. Cancer. Res.* 18(12), 3229–3241 (2012).

26. Saraswathy M, Gong S. Recent developments in the co-delivery of siRNA and small molecule anticancer drugs for cancer treatment. *Materials Today* 17(6), 298–306 (2014).

27. Schiffelers RM, Ansari A, Xu J *et al.* Cancer siRNA therapy by tumor selective delivery with ligand-targeted sterically stabilized nanoparticle. *Nucleic Acids Res.* 32(19), e149–e149 (2004).

28. Zhao P, Wang H, Yu M *et al.* Active Ingredient loaded folic acid targeted nanoparticles of mixed lipid-shell and polymer-core: in vitro and in vivo evaluation. *Eur. J. Pharm. Biopharm.* 81(2), 248–256 (2012).

• **Evaluation technique of lipid core shell-type nanoccarriers.**

29. Zhang L, Zhang L. Lipid–polymer hybrid nanoparticles: synthesis, characterization and applications. *Nano Life* 1(01n02), 163–173 (2010).

30. Patel V, Lalani R, Vhora I *et al.* Co-delivery of Active Ingredient and siRNA through hybrid nanocarrier platform for masking resistance to chemotherapy in lung cancer. *Drug Deliv. Trans. Res.* 1–20 (2020).

31. Win KY, Feng S-S. Effects of particle size and surface coating on cellular uptake of polymeric nanoparticles for oral delivery of anticancer drugs. *Biomater.* 26(15), 2713–2722 (2005).

32. Mandal B, Bhattacharjee H, Mittal N *et al.* Core–shell-type lipid–polymer hybrid nanoparticles as a drug delivery platform. *Nanomed. Nanotechnol.* 9(4), 474–491 (2013).

33. Vhora I, Khatri N, Desai J, Thakkar HP. Caprylate-conjugated Active Ingredient for the development of novel liposomal formulation. *AAPS PharmSciTech* 15(4), 845–857 (2014).

34. Ruozi B, Belletti D, Tombesi A *et al.* AFM, ESEM, TEM, and CLSM in liposomal characterization: a comparative study. *Int. J. of Nanomed.* 6, 557 (2011).

35. Xu P, Van Kirk EA, Li S *et al.* Highly stable core-surface-crosslinked nanoparticles as Active Ingredient carriers for cancer chemotherapy. *Colloids Surf. B Biointerfaces* 48(1), 50–57 (2006).

36. Chougule M, Padhi B, Misra A. Nano-liposomal dry powder inhaler of Active Ingredient: preparation, characterization, and pulmonary pharmacokinetics. *Int. J. Nanomed.* 2(4), 675 (2007).

37. Su W-P, Cheng F-Y, Shieh D-B *et al.* PLGA nanoparticles codeliver Active Ingredient and Stat3 siRNA to overcome cellular resistance in lung cancer cells. *Int. J. Nanomed.* 7, 4269 (2012).

38. Longo-Sorbello GS, Saydam G, Banerjee D, Bertino JR. Cytotoxicity and cell growth assays. In: *Cell Biology.* Elsevier, MA, USA, 315–324 (2006).

39. Patil S, Lalani R, Bhatt P *et al.* Hydroxyethyl substituted linear polyethylenimine for safe and efficient delivery of siRNA therapeutics. *RSC Adv.* 8(62), 35461–35473 (2018).

40. Lee J, Reddy R, Barsky L *et al.* Lung alveolar integrity is compromised by telomere shortening in telomerase-null mice. *Am. J. Physiol. Lung Cell Mol. Physiol.* 296(1), L57–L70 (2009).
41. Fenart L, Casanova A, Dehouck B *et al.* Evaluation of effect of charge and lipid coating on ability of 60-nm nanoparticles to cross an in vitro model of the blood–brain barrier. *J. Pharmacol. Exp. Ther.* 291(3), 1017–1022 (1999).
42. Troutier A-L, Delair T, Pichot C, Ladavière C. Physicochemical and interfacial investigation of lipid/polymer particle assemblies. *Langmuir* 21(4), 1305–1313 (2005).
43. Stavropoulos K. Synthesis and characterization of lipid-polymer hybrid nanoparticles for combinatorial drug delivery [master's thesis] (2011). https://core.ac.uk/download/pdf/213394887.pdf
44. Thevenot J, Troutier A-L, David L *et al.* Steric stabilization of lipid/polymer particle assemblies by poly (ethylene glycol)-lipids. *Biomacromolecules* 8(11), 3651–3660 (2007).
45. Lim SK, De Hoog H-P, Parikh AN *et al.* Hybrid, nanoscale phospholipid/block copolymer vesicles. *Polymers* 5(3), 1102–1114 (2013).
46. Li J, Wang X, Zhang T *et al.* A review on phospholipids and their main applications in drug delivery systems. *Asian J. Pharm. Sci.* 10(2), 81–98 (2015).
47. Khatri N, Rathi M, Baradia D, Misra A. cRGD grafted siRNA nano-constructs for chemosensitization of Active Ingredient hydrochloride in lung cancer treatment. *Pharm. Res.* 32(3), 806–818 (2015).
48. Zhao Y, Lu H, Yan A *et al.* ABCC3 as a marker for multidrug resistance in non-small cell lung cancer. *Sci. Rep.* 3, 3120 (2013).
49. Rabanel J-M, Hildgen P, Banquy X. Assessment of PEG on polymeric particles surface, a key step in drug carrier translation. *J. Control. Release.* 185, 71–87 (2014).
50. Blanco E, Shen H, Ferrari M. Nanoparticle rational design implementation for overcoming delivery barriers. *Nat Biotechnol.* 33, 941–951 (2015).
51. Nakamura K, Yamashita K, Itoh Y *et al.* Comparative studies of polyethylene glycol-modified liposomes prepared using different PEG-modification methods. *Biochim. Biophys. Acta Biomembr.* 1818(11), 2801–2807 (2012).
52. Zhang L, Hu Y, Jiang X *et al.* Camptothecin derivative-loaded poly (caprolactone-co-lactide)-b-PEG-b-poly (caprolactone-co-lactide) nanoparticles and their biodistribution in mice. *J. Control. Release.* 96(1), 135–148 (2004).
53. Li X, Li R, Qian X *et al.* Superior antitumor efficiency of Active Ingredient-loaded nanoparticles by intratumoral delivery with decreased tumor metabolism rate. *Eur. J. Pharm. Biopharm.* 70(3), 726–734 (2008).
54. Zarogoulidis P, Chatzaki E, Porpodis K *et al.* Inhaled chemotherapy in lung cancer: future concept of nanomedicine. *Int. J. Nanomed.* 7, 1551 (2012).
55. Kaialy W, Nokhodchi A. Freeze-dried Active Ingredient for superior pulmonary drug delivery via dry powder inhaler. *Pharm. Res.* 30(2), 458–477 (2013).
56. Chougule MB, Padhi BK, Jinturkar KA, Misra A. Development of dry powder inhalers. *Recent Pat. Drug Deliv. Formul.* 1(1), 11–21 (2007).
57. Allison SD, Molina MDC, Anchordoquy TJ. Stabilization of lipid/DNA complexes during the freezing step of the lyophilization process: the particle isolation hypothesis. *Biochim Biophy Acta Biomembr.* 1468(1), 127–138 (2000).
58. Nishiyama N, Okazaki S, Cabral H *et al.* Novel Active Ingredient-incorporated polymeric micelles can eradicate solid tumors in mice. *Cancer Res.* 63(24), 8977–8983 (2003).
59. Gryparis EC, Hatziapostolou M, Papadimitriou E, Avgoustakis K. Anticancer activity of Active Ingredient-loaded PLGA-mPEG nanoparticles on LNCaP prostate cancer cells. *Eur. J. Pharm. Biopharm.* 67(1), 1–8 (2007).
60. Khatri N, Rathi MN, Baradia D, Trehan S, Misra A. In vivo delivery aspects of miRNA, shRNA and siRNA. *Crit. Rev. Ther. Drug Carrier Syst.* 29(6), 487–527 (2012).
61. Nillawar AN, Bardapurkar J, Bardapurkar S. High sensitive C-reactive protein as a systemic inflammatory marker and LDH-3 isoenzyme in chronic obstructive pulmonary disease. *Lung India.* 29(1), 24 (2012).